Modeling of Fading Figure for Non-Stationary Indoor Radio Channels

Hassan El-Sallabi and Abdulaziz Aldosari
Department of Technical Affairs, QAF
Qatar

Qammer H. Abbasi
Department of Electrical and Computer Engineering,
Texas A&M University at Qatar
Qatar

Abstract - Fading models of practical mobile radio channel may change over time and/or due to mobility being Rice, Rayleigh, double-Rayleigh, etc, depending on the nature of radio wave propagation, which results in a non-stationary channel. This work is based on investigation of fading figure (FF) that addresses non-stationarity nature of radio channels. The FF is represented by the parameter m of Nakagami-m distribution. For an indoor environment system, our results show the parameter m, which can be modeled as a generalized extreme value distribution. . The statistical distribution model of parameter m can be used to study performance of wireless communication system under non-stationary radio channels.

Key words: non-stationary, radio channel, amount of fading, Nakagami-m, BER.

I. INTRODUCTION

Due to demand of continuous connection with high data rate services that require wireless devices, such as smartphones to be always on for long time with mobility which makes the radio channels nature non-stationary. This require careful consideration for proper radio channel modeling that addresses the non-stationarity behavior. In mobile radio channels, as the mobile terminal moves, it experiences different fading conditions. These fading conditions vary with nature of multipath components; 1) whether line of sight exist or not; 2) variability of number of strong components with diffuse scattering components. So, a real world fading channel for mobile terminal could be a combination of different fading channel types that changes over time and mobility. Different fading models have been developed and utilized in literature such as Rician, Rayleigh, etc. However, it has also been found that, in some environments, fading does not follow Rician or Rayleigh distributions but more severe fading than Rayleigh [1] such as the well-known non-stationary behavior of vehicle-to-vehicle channels [2,3,4], where both platforms are mobile in addition to low antenna heights for both ends. Due to complexity of multipath channels, there are still many issues that are not addressed, e.g., proper modeling of fading conditions of variable number of strong components with available diffuse channel components except for few recent results appear in [5,6] and proper modeling of non-stationary channels and how it switches from fading channel type to another.

In this work, we focus on modeling of FF as channel fading measure that did not receive detailed investigations in channel modeling research. It provides information about fading levels by describing it by one index value that can be considered relative to Rayleigh fading, i.e., *FF*=1. This work assumes that non-stationary fading channel has a distribution of its fading amplitudes varies with channel condition. This variability is modeled via modelling parameter $m \geq 0.5$ that covers fading degrees from very severe fading conditions, i.e., $m \approx 0.5$, till no fading conditions, i.e., $m \to \infty$. The paper is organized as follows: Section II describes the fading figure, Section III presents channel model used in the study and Section IV discusses numerical results of the work. Conclusion of this work is presented in Section IV.

II. FADING FIGURE

Fading channels are modeled based on their amplitude fading distribution using different models such as Rayleigh, double Rayleigh, Rician, Nakagami, etc. In this work, non-stationary radio channels are defined by variable fading types that are usually represented by different fading models. In such scenarios, it is important to adopt a measure as index of severity of fading level that can be used to describe fading depth without a need to revert to a fading type or a model. Hence, the non-stationarity nature of fading type can be described by a variable fading index, denoted as fading figure. One of the known descriptive statistics to dispersion measures of variability of data is the coefficient of variation (CV). It quantifies variability level of data given as a series of numbers, independent of the unit of measurement for these numbers [7]. This coefficient has no unit by definition since it is computed as a ratio of standard deviation (σ) of the data to its mean (μ) (i.e., $CV = \frac{\sigma}{\mu}$). This work is based on considering Rayleigh fading channel as a benchmark, whether the channel fading conditions are hyper-Rayleigh, Rayleigh, or less than Rayleigh. However, due to ease of mathematical convenience and tractability, instead of using CV, it is quite common in statistics to use squared coefficient of variation (SCV), which is defined as [7]

$$\mathrm{SCV} = \frac{Var}{\mu^2} = \frac{E\left((x-\mu)^2\right)}{\mu^2} = \frac{E(x^2)}{\left(E(x)\right)^2} - 1 \qquad (1)$$

where x is a random variable, $E(\cdot)$ is expectation operator.

Fading channel can be characterized by a random variable α that describes random nature of envelope fading. Since the performance of wireless communication systems is mainly function of signal to noise ratio, the fading level has to be described in power, i.e., α^2. Hence, Rayleigh amplitude fading channels can be described as exponential fading distribution in power domain. The SCV of received signal power characterizes the amount of fading of signal power as follows

$$SCV = \frac{var(\alpha^2)}{\left(E(\alpha^2)\right)^2} \quad (3)$$

This has been presented in [8] and called amount of fading. The exponential statistical distribution has a feature that its variance is equal to its mean squared, which means that for Rayleigh fading channel, whose power of received signal has exponential distribution, the $SCV = 1$. For Nakagami-m fading channel, which is known to be applicable to model different propagation environments, the probability density function (PDF) of instantaneous received power follows Gamma distribution, which can be written as

$$p(x) = \frac{\beta^m}{\Gamma(m)} x^{m-1} e^{-\beta x} \quad (4)$$

where m and β are known as shape and inverse scale parameters. The mean of Gamma distributed random variable is m/β and its variance is m/β^2 resulting to $SCV = \frac{1}{m}$; which relates the SCV to parameter m of Nakagami-m fading channel. Then, the fading figure, parameter m, can be estimated from inverse of SCV as follows:

$$m = \frac{\left(E(\alpha^2)\right)^2}{var(\alpha^2)} \quad (5)$$

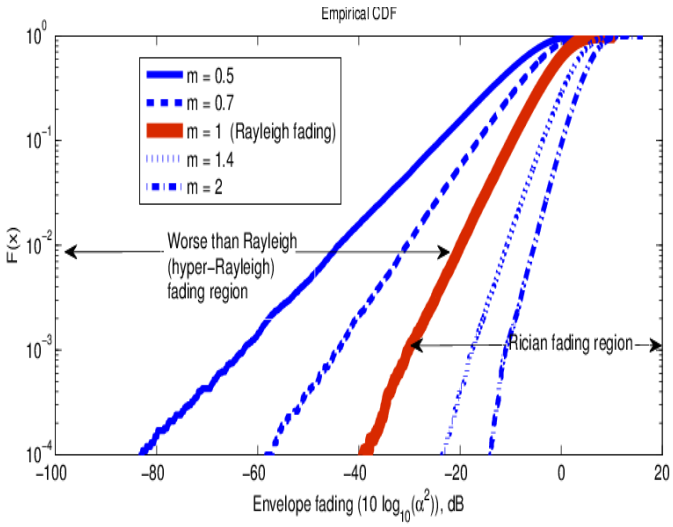

Figure 1. Severity of fading level of different fading channels.

It is known that if $m = 1$, the Gamma distribution reverts to exponential distribution. This corresponds to $SCV = 1$, which is the amount of fading (AF) of instantaneous received power of exponential distribution that results from Rayleigh envelop fading channel. Hence, the parameter m of Nakagami-m distribution as a fading figure can be used via AF to describe the fading degree (or level) experienced by a signal propagates in multipath channel as illustrated in Figure 1. If m=1, the envelop fading channel follows Rayleigh distribution. If m<1, then the fading is considered to hyper-Rayleigh fading. For example, when m = 0.5, the fading channel is considered to be severest fading channel in this analysis, which corresponds to one-side Gaussian fading channel, i.e., Nakagami-q envelop distribution with q = 0. If m>1, the fading channel is considered less severe than Rayleigh and as m increases, it becomes more Rician fading. If $m \to \infty$, the channel becomes non-fading.

III. Radio Channel Model

Channel characteristics that are related to non-stationarity nature of radio channel, can be extracted by either mobile channel measurement data or simulated radio channel with a model based on electromagnetic theory. The used radio channel model in this investigation is physics-based that take into account signal interaction with scatterers identified with specific propagation mechanisms. The model is based on multi-ray propagation derived from image theory. Each ray is characterized in multi-dimensions; delay azimuthal and co-elevation arrival angle, azimuthal and co-elevation departure angle. The angular information are needed to consider the interplay between rays and volume of antenna patterns at transmitter and receiver ends. These ray parameters are derived based on locations of transmitter and receiver with respect to positions of scatterers as defined by the geometry of the environment. The derivation is based on utilizing vector mathematical operations. It follows same approach adopted in [10,11] and extending them to indoor propagation environment. The amplitude of each ray is calculated by considering free space loss and interaction attenuation of each electromagnetic (EM) wave with scatterers. The channel transfer function of the radio channel, $H(t,f)$, can be obtained as a linear superposition of N individual rays represented as follows:

$$H(t,f) = \sum_{n=0}^{N} H_n(t,f)$$

where $H_n(t,f)$ is the radio channel transfer function for individual ray n, where n =0 is for line of sight (LOS) ray, if exists, and n>0 is for rays that undergo propagation mechanisms other than LOS. The formulation can be further detailed as follows

$$H(t,f) = \frac{\lambda}{4\pi r_{los}} \sqrt{G_{tx}(\varphi_{los}, \vartheta_{los}) G_{rx}(\phi_{los}, \theta_{los})} \times \delta(t - \tau_{los}) e^{-jk(r_{los} - \mathbf{V}\cdot\mathbf{\Psi}_{los} t)} + \sum_{n=1}^{N} \frac{\lambda}{4\pi r_n} \sqrt{G_{tx}(\varphi_n, \vartheta_n) G_{rx}(\phi_n, \theta_n)} \prod_{p=1}^{P_n} \Gamma_p e^{-jkd_{n,p}} \times \delta(t - \tau_n) e^{jk(\mathbf{V}\cdot\mathbf{\Psi}_n t)}$$

where λ is the wavelength of operating frequency f, k is the wave number expressed as $k = \frac{2\pi}{\lambda}$, $G_{tx}(\varphi_n, \vartheta_n)$, $G_{rx}(\phi_n, \theta_n)$ are the transmitter and receiver antenna gain, respectively, Γ_p denotes the Fresnel reflection coefficient for the *p-th* wave-interface intersection, $\mathbf{V}$ is the velocity of the mobile terminal, which is assumed as the receiver in this notation, and defined by $\mathbf{V} = v_x\vec{x} + v_y\vec{y} + v_z\vec{z}$ and $\boldsymbol{\Psi_n}$ stands for the arrival direction vector defined for ray *n* as

$$\boldsymbol{\Psi}_n = \cos(\phi_n)\sin(\theta_n)\,\vec{x} + \sin(\phi_n)\sin(\theta_n)\,\vec{y} + \cos(\theta_n)\vec{z}$$

where ϕ_n and θ_n are the horizontal and co-elevation arrival angles of ray *n* (or LOS ray when subscript is los) relative to the *x*-axis and z-axis, respectively, r_{los} is the length of LOS path, $d_{n,p}$ denotes the distance traversed by the specular wave between the (p - 1) and p-th boundary intersections, and r_n is the specular reflection path length.

To estimate fading figure, parameter *m,* from simulated radio channels, it is needed to extract the envelope of the channel fading. The radio channel has mainly three effects on received signal, which are path loss, shadow fading and small scale fading. The three channel components results from complex sum of all rays, while the first two components (i.e., path loss and shadow fading) can be obtained from sum of powers of all rays. Hence, the channel fading envelope can be obtained as follows

$$\alpha(t,f) = \frac{|\sum_{n=0}^{N} H_n(t,f)|}{\sqrt{\sum_{n=0}^{N}|H_n(t,f)|^2}}$$

Figure 2 depicts the path gain of the simulated LOS propagation channel, when both power of complex sum of received signals that show small scale fading variation due to constructive and destructive interferences. The sum of powers of rays represent the path loss and shadowing is shown in pink color, i.e., solid thick line. Then, $\alpha(t,f)$ can be obtained from square root of the ratio of power of sum of complex signals to sum of powers of received rays. If measurement data is available, then α can be obtained by processing measurement data by smoothing out small-scale fading over selected window length to get the path loss and shadow fading component. Then, estimated large scale fading components are subtracted from the original data to extract the channel envelope (or signal envelope) components as they represent the remaining fast fading component.

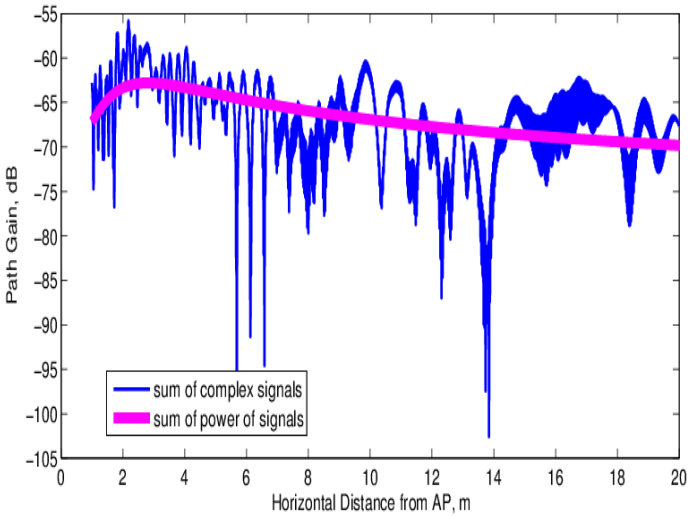

Figure 2. Path gain of the simulated LOS propagation channel.

IV. Numerical Results

This work simulates corridor indoor environment to find variability of fading figure that indicates non-stationary radio channel. The corridor with dimensions: H = 3.5 m, W = 2 m, and L = 30 m. Simulated radio channel is at frequency range 5 GHz and bandwidth is 80 MHz, which correspond to parameters of IEEE802.11ac system. The antenna height of receiver, *i.e.* mobile client, is 1.7 m, which has a speed of about 1 m/s. The height of transmitter, *i.e.* access point, is on ceiling. In addition to line of sight component, multiple specular reflections are included, where number of images per surface is assumed five. The multiple reflection rays result from different combinations of bouncing between walls, ceiling and ground of more than five. The electrical properties of reflection surfaced are given in terms relative permittivity, which is assumed to be 5, while the conductivity is assumed 0.02. The antenna pattern is omnidirectional, which has the well-known donut shape in its three dimensional pattern. It is assumed that transmitter and receiver antennas are vertically polarized. Multi-dimensional channel transfer functions for every spatial location are simulated. The simulation is for a client station travelled a path starting from a horizontal distance of a route length of about 20 m of staring from 1 m from AP with almost continuous spatial resolution of 0.04 cm, which corresponds to 3167 sampled spatial point. The simulated temporal range is for one second for every spatial location. The temporal sampling rate is 26,000 samples/sec. As a result of movement of client station, the differential spacing between the multipath components changes too with spatial variant and mobile terminal speed. The parameter *m* as a measure of fading severity is estimated as described earlier. Figure 3 shows variability of parameter *m* as a function of distance. Though the simulated channel is LOS with multipath

propagation, it is evident from Figure 3 that fading figure varies significantly from strong Rician channel ($m \gg 1$) to Rayleigh fading channel ($m \approx 1$) and hyper-Rayleigh channel ($m < 1$), i.e., $m \approx 0.33$ for double-Rayleigh fading and $m \approx 0.5$ for single-sided Guassian fading.

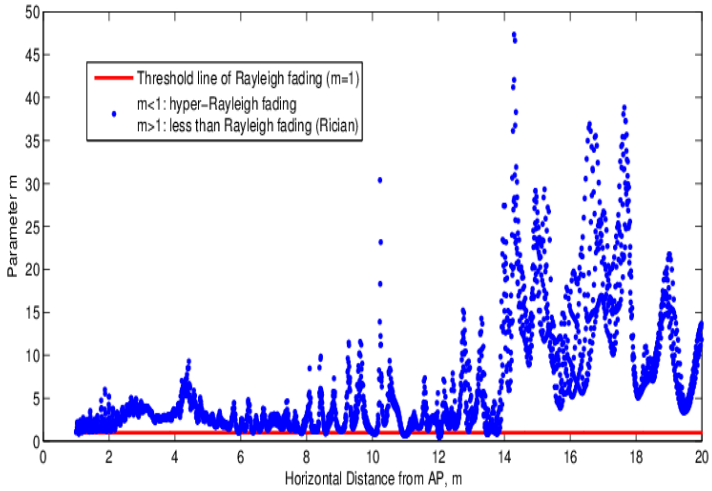

Figure 3. Variation of fading figure with distance.

This can be explained by variable interplay of multipath components with antenna pattern and differential differences between path lengths as well as different levels of reflection losses make the interference between multipath components differ with spatial movement of client station. For example, for short distance from AP, the LOS component could be heavily attenuated by antenna pattern due to large elevation angles effect. There are channel conditions, where many comparatively strong multipath components make that channel not to be dominant by a single LOS component. This moves the channel fading conditions to other fading types than Rician. This cause channel envelope to follow different values of parameter *m*. Each value of parameter *m* is estimated from a time series of one second. The variability of parameter *m* from as low as close to 0.5 and as high as close to 40 to indicate that channel experience wide range of fading types. Figure 4 shows envelop distribution at different ranges of parameter *m* and their corresponding fitted statistical distributions and their approximation with Nakagami-*m* distribution for the corresponding values of parameter *m*. For low range of m ($m \approx 0.5$), the fading level is severe as can be seen from the PDF shown in Figure 4a. This corresponds to what we call it hyper-Rayleigh fading and worst fading type know as one-sided Gaussian distribution. Figure 4b depicts the case when $m \approx 1$, which is clearly Rayleigh fading approximation as can be seen in fitted Rayleight statistical model. The third case for $m>1$ is shown in Figure 4c, which corresponds to scenario for less than Rayleigh fading, i.e., Rician fading channel.

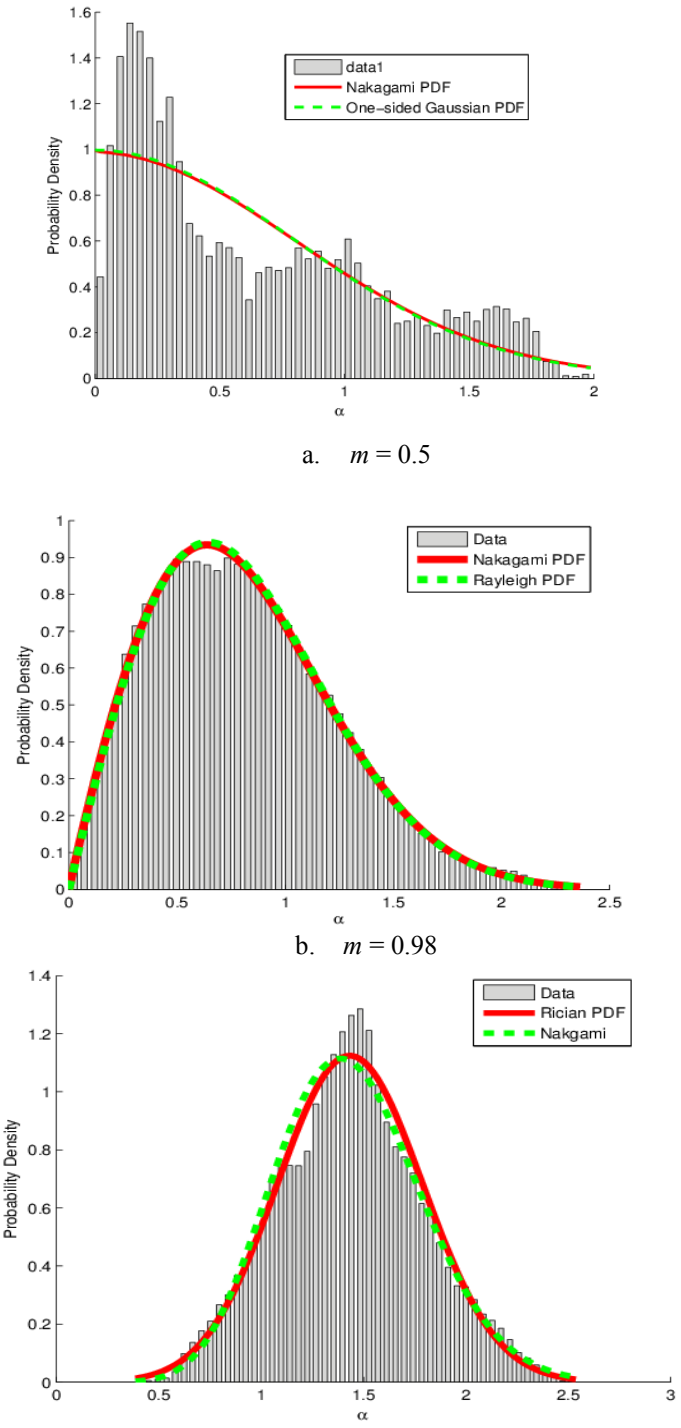

a. $m = 0.5$

b. $m = 0.98$

c. $m = 4.2$

Figure 4. Envelop distributions at different values of parameter m.

To account for non-stationarity of radio channel, the variability of parameter *m* should be modeled with a statistical distribution

that can be used in studying impact of variation of this parameter on non-stationarity of the channels. Then, empirical statistical distribution for of parameter *m* computed at all spatial locations is obtained for fitting their proper parametric statistical distribution model. The empirical probability density function has been tested for fitting against different statistical distribution to select the best fitting parametric model of statistical distributions. The tested statistical distributions are normal, lognormal, exponential, gamma, logistic, loglogistic, uniform, weibull, extreme values, generalized pareto, generalized extreme value, inverse Gaussian, Nakagami-m, and Rayleigh. The decision of selection the statistical distribution is based on results of likelihood value of maximum likelihood estimator for 95% confidence interval. These values are assessed to check the fitting results of every statistical distribution listed earlier. Akaike information criterion is also an option but we used log-likelihood criterion, which may have any value that allows comparing fitting of different statistical distributions and the maximum likelihood solution can be used for most (or about every) parametric statistical distribution models. It is not restricted to normally distributed errors as it is associated with uncertainty. The selection is to pick the model that has maximum likelihood. Figure 5 shows empirical probability density function of parameter *m* for the tested environment. The fit experiments show the generalized extreme value (GEV) distribution has best fit. The estimation of parameter *m* is sensitive to extreme values in their sample data. The extreme value distribution arises from extreme values (maxima or minima) in sample data, which is unlike normal distribution that arises from central limit theorem on sample averages of data. The GEV distribution is a family of statistical distributions that combines Gumbel, Fréchet and Weibull statistical distributions. They are also known as type I, II, and III extreme value distribution. Extreme value theory originally is used as a framework to analyze the tail behavior of statistical distributions in different applications. In this work, we do not really model the extreme values themselves but try to model a parameter that is affected by extreme values of the radio channel such as deep fades. The probability density function (PDF) of the GEV distribution can be expressed [12] for $k \neq 0$ as

$$f(x;\sigma,\mu,k) = \frac{\left(\frac{1}{\sigma}\right)\exp\left(-\left(1+k\frac{(x-\mu)^{-\frac{1}{k}}}{\sigma}\right)\right)}{\left(1+k\frac{(x-\mu)}{\sigma}\right)^{1+\frac{1}{k}}}$$

For $\left\{1+k\left(x-\frac{\mu}{\sigma}\right)\right\} > 0$ and for $k = 0$, the PDF is given as

$$f(x;\sigma,\mu,k) = \left(\frac{1}{\sigma}\right)\exp\left(-\exp\left(-\frac{(x-\mu)}{\sigma}\right)-\frac{(x-\mu)}{\sigma}\right)$$

Based on value of *k,* different statistical distributions result; when $k \to 0$, $k > 0$, and $k < 0$, the GEV distribution becomes Gumbel, Weibull and Fréchet distributions, respectively. The parameter *k* is called shape factor, μ is location parameter and σ is scaling parameter. The fitting results shown in Figure 5 that lead to selection of GEV distribution are $k = 0.93$ $\mu = 2.04$, and $\sigma = 1.72$.

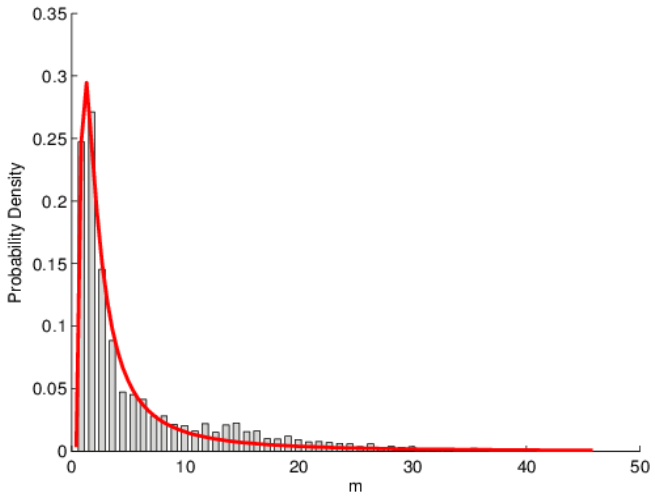

Figure 5. Empirical probability density function of parameter m fitted to GEV distribution.

V. Conclusion

This work addresses non-stationary radio channels and how they vary from fading type to other. The variability of fading type is measured with a fading figure in terms of parameter-m of Nakagami-*m* fading channel model. The parameter *m* is related through mapping functions to different parameters of fading statistical distributions; e.g., Rayleigh, Rician, one-sided Gaussian distributions, etc. The fading figure for tested indoor propagation environment is modeled in a generalized extreme value statistical distribution to account for variability of fading channel types. The proposed distribution can be used to study performance of wireless communication system under scenarios of non-stationary radio channels.

References

[1] I. Sen, D. W. Matolak, and W. Xiong, "Wireless channels that exhibit 'worse than Rayleigh' fading: Analytical and measurement results*," in Proc. IEEE MILCOM*, Oct. 2006, pp. 1–7.

[2] O. Renaudin, V. M. Kolmonen, P. Vainikainen, and C. Oestges, "Nonstationary narrowband MIMO inter-vehicle channel characterization in the 5 GHz band," *IEEE Trans. Veh. Technol.*, vol. 59, no. 4, pp. 2007– 2015, May 2010.

[3] L. Bernadó, T. Zemen, J. Karedal, A. Paier, A. Thiel, O. Klemp, N. Czink, F. Tufvesson, A. F. Molisch, and C. F. Mecklenbräuker, "Time-, frequency-, and space-varying k-factor analysis of V2V street crossing radio channels," *in Proc. IEEE Int. Symp. PIMRC*, Sep. 2010, pp. 58–63.

[4] L. Bernado, T. Zemen, F. Tufvesson, A.F. Molisch, C.F. Mecklenbrauker, Timeand frequency-varying K-factor of non-stationary vehicular channels for safety relevant scenarios, arXiv:1306.3914, 2014.

[5] N.C. Beaulieu and X. Jiandong "Novel Fading Model for Channels With Multiple Dominant Specular Components*," IEEE Wireless Communications Letters*, IEEE EARLY ACCESS ARTICLES, 2014.

[6] M. Rao, F.J. Lopez-Martinez, M-S Alouini, and A. Goldsmith "MGF Approach to the Analysis of Generalized Two-Ray Fading Models," *IEEE Transactions on Wireless Communications*, IEEE EARLY ACCESS ARTICLES, 2015

[7] H. Abdi, "Coefficient of variation" in Salkind, N.J., Dougherty, D.M., Frey, B. (Eds.), Encyclopedia of Research Design. SAGE Publications, Inc., Thousand Oaks, CA, pp. 169–171

[8] U. Charash, "Reception through Nakagami fading multipath channels with random delays," *IEEE Trans. Commun.*, vol. 27, pp. 657–670, Apr. 1979.

[9] M. Simon and M. Alouini, *Digital Communications over Fading Channels: A Unified Approach to Performance Analysis*, John Wiley & Sons, Inc. 2000.

[10] H.M. El-Sallabi and P. Vainikainen "Physical modeling of line-of-sight wideband propagation in a city street for microcellular communication," *Journal of Electromag-netic Waves and Applications* 14, 2000, pages 905-927.

[11] H.M. El-Sallabi and P. Vainikainen, "Radio wave propagation in perpendicular streets of urban street grid for microcellular communications. Part I: Channel modeling," *Progress In Electromagnetics Research* (*PIER*) 40, pages 229-254.

[12] D. Walshaw, *Generalized Extreme Value Distribution,* John Wiley & Sons, Ltd, 2013.